Toll-like receptor 8 functions as a negative regulator of neurite outgrowth and inducer of neuronal apoptosis

Yinghua Ma,[1,2,3] Jianxue Li,[1] Isaac Chiu,[4] Yawen Wang,[1,2,3] Jacob A. Sloane,[1,2,3] Jining Lü,[5] Bela Kosaras,[1] Richard L. Sidman,[1,2] Joseph J. Volpe,[2,6] and Timothy Vartanian[1,2,3]

[1]Department of Neurology, Beth Israel Deaconess Medical Center, Boston, MA 02115
[2]Program in Neuroscience, [3]Center for Neurodegeneration and Repair, and [4]Center for Blood Research, Graduate Program in Immunology, Harvard Medical School, Boston, MA 02115
[5]Pulmonary Center, Boston University School of Medicine, Boston, MA 02118
[6]Department of Neurology, Children's Hospital, Boston, MA 02115

Toll receptors in *Drosophila melanogaster* function in morphogenesis and host defense. Mammalian orthologues of Toll, the Toll-like receptors (TLRs), have been studied extensively for their essential functions in controlling innate and adaptive immune responses. We report that TLR8 is dynamically expressed during mouse brain development and localizes to neurons and axons. Agonist stimulation of TLR8 in cultured cortical neurons causes inhibition of neurite outgrowth and induces apoptosis in a dissociable manner. Our evidence indicates that such TLR8-mediated neuronal responses do not involve the canonical TLR–NF-κB signaling pathway. These findings reveal novel functions for TLR8 in the mammalian nervous system that are distinct from the classical role of TLRs in immunity.

Introduction

TLRs are perhaps the best-studied pathogen-recognition receptors in mammals, and they serve essential functions in mediating innate immunity and establishing adaptive immunity (Akira and Takeda, 2004). TLRs specifically recognize a wide array of microbial components, referred to as pathogen-associated molecular patterns (PAMPs), and upon activation, they engage a signaling pathway leading to proinflammatory responses against pathogenic infection. In addition to a well-described role in immunity (Hoffmann, 2003), Toll, which is the *Drosophila melanogaster* orthologue of the TLRs, plays crucial roles in establishing the dorsoventral axis polarity during embryogenesis (Belvin and Anderson, 1996), in synaptogenesis, and in axon pathfinding (Rose et al., 1997). Such nonimmune functions of this receptor family remain undiscovered in mammals, despite the fact that TLRs are evolutionarily conserved across species (Hoffmann et al., 1999).

In the mammalian central nervous system (CNS), TLRs are expressed in microglia and astrocytes and activate inflammatory pathways in response to pathogenic infection, sterile tissue injury, or in neurodegeneration (Lehnardt et al., 2003; Kielian, 2006). The expression of certain TLRs has been recently documented in mammalian neurons (Prehaud et al., 2005; Wadachi and Hargreaves, 2006), but the functional significance in this cell type has yet to be elucidated. In this study, we define the expression and localization of TLR8 in mouse neurons and reveal the dissociable roles for TLR8 in neurite outgrowth and neuronal apoptosis.

Correspondence to Timothy Vartanian: tvartani@bidmc.harvard.edu

Abbreviations used in this paper: CNS, central nervous system; DIG, digoxin; DIV, days in vitro; E, embryonic day; IRAK, interleukin-1 receptor–associated kinase; LPS, lipopolysaccharide; NF-κB, nuclear factor-κB; P, postnatal day; PAMPs, pathogen-associated molecular patterns; TLRs, Toll-like receptors.

The online version of this article contains supplemental material.

Results and discussion

Western-blot analysis for TLRs within the developing mouse brain revealed a unique expression profile for TLR8. TLR8 expression in brain (Fig. 1 A) was detected by embryonic day 12 (E12), increased in late embryonic and neonatal stages, and then declined drastically after postnatal day 21 (P21), which is when the basic patterns of neurogenesis and axonogenesis are complete. In adult brain, TLR8 expression is low, but detectable (Fig. 1 A). The remarkable abundance of TLR8 in embryonic brains, and its developmentally regulated expression, was unexpected because mammalian TLRs are thought to be expressed predominantly in pathogen-sensing tissues and to function in immunity.

Supplemental material can be found at:
http://doi.org/10.1083/jcb.200606016

The Journal of Cell Biology, Vol. 175, No. 2, October 23, 2006 209–215
http://www.jcb.org/cgi/doi/10.1083/jcb.200606016

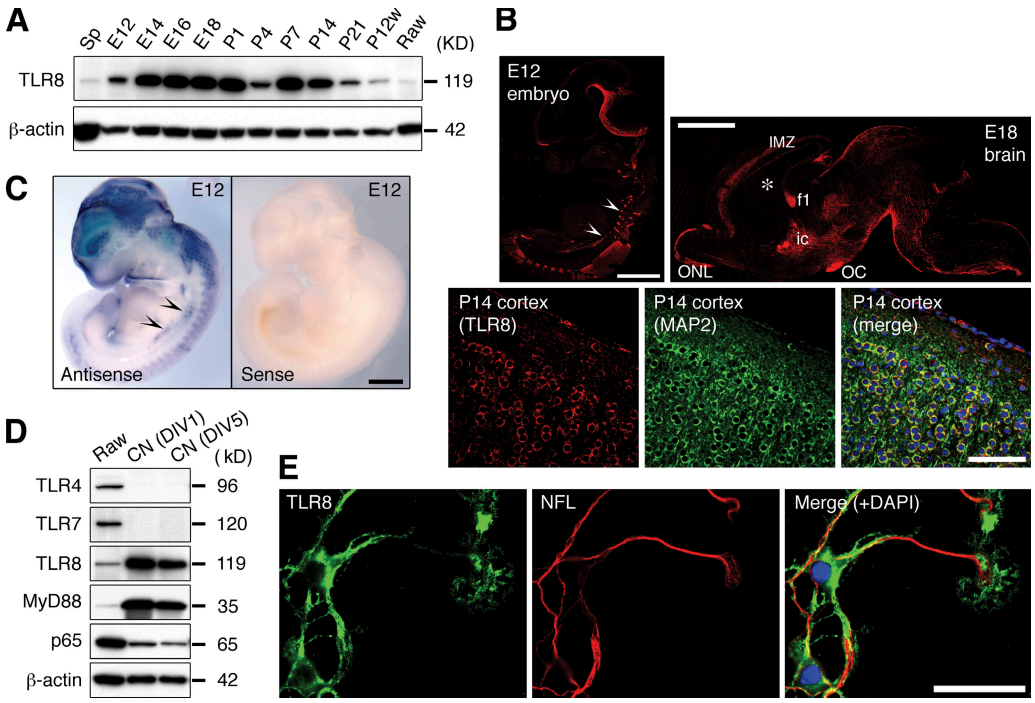

Figure 1. **TLR8 is dynamically expressed during mouse brain development and localizes to axons and neurons.** (A) Western blot analysis of TLR8 expression in the developing mouse brains. Spleen (Sp) and Raw264.7 (Raw) macrophages are positive controls for anti-TLR8 immunoreactivity. β-actin serves as loading control. (B) Immunohistochemical analysis of TLR8 expression in sagittal sections of E12 embryo, E18 brain, and P14 cerebral cortex. The images of the E12 embryo and E18 brain were acquired by confocal microscopy using the Tile Scan function. (C) Whole-mount in situ hybridization of E12 embryo using a digoxin (DIG)-labeled probe specific to *Tlr8* mRNA. Arrowheads in B and C indicate the sympathetic nerve trunk. (D) Western blotting of TLR4, TLR7, TLR8, MyD88, and NF-κB subunit p65 in cortical neurons cultured for 1 (DIV1) and 5 d (DIV5). (E) Immunocytochemistry of TLR8 in cultured cortical neurons. MAP2 and neurofilament 200 kD (NFL) are neuron-specific markers. An affinity-purified anti-TLR8 polyclonal antibody was used in A, B, D, and E. P, postnatal day; P12w, 12-wk-old; ic, internal capsule; IMZ, cortical intermediate zone; f1, fimbria of hippocampus, OC, optic chiasm, ONL, olfactory nerve layer. Bars: (B, top, and C) 1 mm; (B, bottom) 100 μm; (E) 50 μm.

We further examined the expression pattern of TLR8 in the developing mouse nervous system by immunohistochemistry with an anti-TLR8 polyclonal antibody whose specificity we verified by human embryonic kidney cell transfection and antibody absorption (Fig. S1 A, available at http://www.jcb.org/cgi/content/full/jcb.200606016/DC1). In early embryos, TLR8 is highly expressed in peripheral sensory and sympathetic ganglia and in postmitotic migrating CNS cells, but not in the periventricular cell proliferation zones (Fig. 1 B and Fig. S1 A, c). Whole-mount in situ hybridization with a *Tlr8*-specific probe yielded an mRNA distribution signal at E12 that closely approximates the immunostaining pattern (Fig. 1 C). TLR8 expression in late embryonic brains was sharply restricted to axonal tracts, including the olfactory nerve fiber layer, cortical intermediate zone, internal capsule, anterior commissure, fimbria of hippocampus, optic chiasm, and other major fiber systems (Fig. 1 B and Fig. S1 B). Postnatally, TLR8 is diffusely expressed in most regions of the brain and localizes mainly to neuronal somata (Fig. 1 B). This dynamically changing spatiotemporal expression pattern implies a role for TLR8 in development of the mammalian nervous system.

In neurons isolated from E16 mouse neocortex, TLR8 is expressed at a markedly higher level than in macrophages (Fig. 1 D). TLR8 in cultured cortical neurons localizes to the perinuclear cytoplasm and neurites, including their growth cones (Fig. 1 E). The myeloid differentiation factor 88 (MyD88), which is an essential adaptor protein for signaling through all TLRs, except for TLR3 (Akira and Takeda, 2004), was also detected in cortical neurons (Fig. 1 D). TLR4 is not present in cortical neurons (Fig. 1 D), as we previously reported (Lehnardt et al., 2003), and indicates the purity of our neuronal cultures, as microglia are known to express high levels of TLR4 (Lehnardt et al., 2003). It is noteworthy that TLR7, a TLR family member phylogenetically and structurally related to TLR8 (Du et al., 2000), is not expressed by neurons (Fig. 1 D).

Mouse TLR8 was previously suggested to be nonfunctional, based on the observation that ligand stimulation of human, but not mouse, TLR8 induces NF-κB activation (Jurk et al., 2002). Because the *Tlr8* genomic locus is conserved between human and mouse (Roach et al., 2005), and because the amino acid residues within the TIR domain critical to TLR signaling are identical between human and mouse TLR8 (unpublished data), the mechanism underlying such a species-dependent NF-κB activation by TLR8 remains unclear. However, the inability of mouse TLR8 to activate NF-κB does not necessarily infer a lack of function, as TLR8 may function in biological processes that do not require NF-κB activation, or may alternatively operate in a cell type–specific manner.

To investigate the function of TLR8 in neurons, we analyzed the morphological response of freshly plated cortical neurons to a highly permeable synthetic compound, resiquimod (R-848). Although it is a dual TLR7 and TLR8 agonist (Jurk et al., 2002),

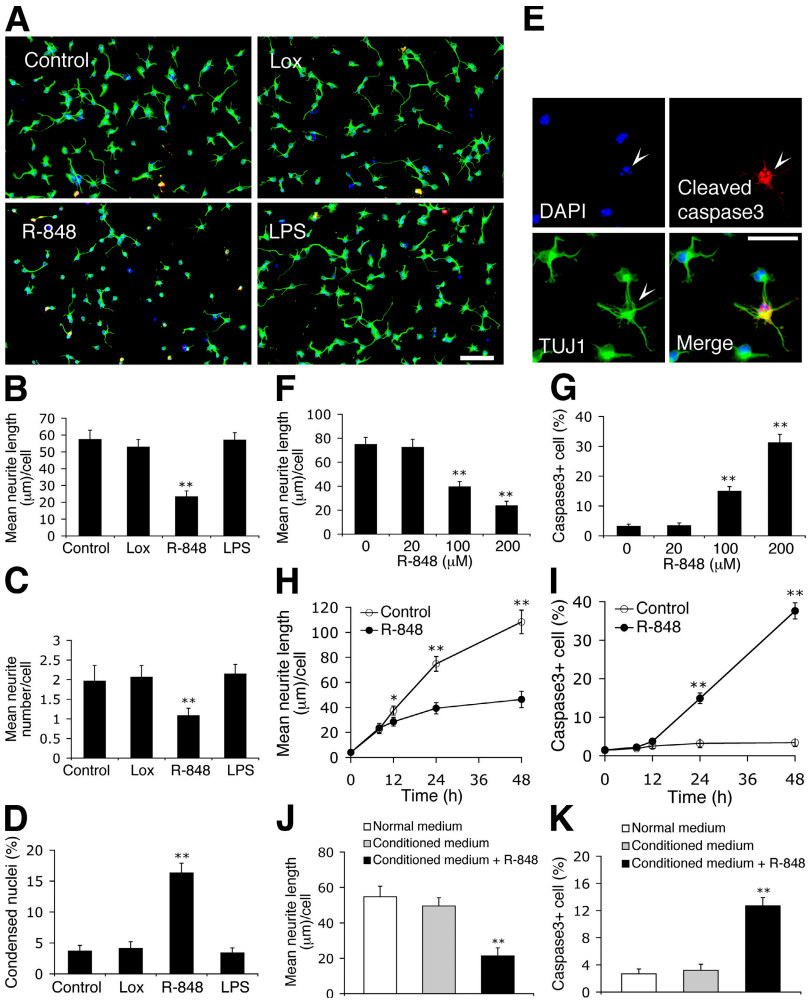

Figure 2. **R-848 inhibits neurite outgrowth and triggers apoptosis in freshly cultured cortical neurons.** (A) Representative micrographs of neurons untreated (control) or treated with 500 μM loxoribine (Lox; TLR7 agonist), 100 μM R-848 (TLR7/8 agonist), or 5 μg/ml LPS (TLR4 agonist) for 24 h. Cells were fixed and double-immunostained with anti–βIII-tubulin (green) and anti-cleaved caspase3 (red) monoclonal antibodies. (B–D) Quantification of the effects of PAMPs on neurite length (B), neurite number (C), and cell death (D) as characterized by condensed nuclei ($<50 \pm 25$ μm^2). (E) Representative micrographs of R-848–treated cultures show a neuron (βIII-tubulin/TUJ1) with a condensed nucleus (DAPI; arrowhead) stained by anti-cleaved caspase3. Dose–response curve (F and G) and time-course (H and I) of R-848 effects on neurite outgrowth (F and H) and apoptosis (G and I). In F and G, neurons were treated for 24 h; in H and I, neurons were exposed to 100 μM R-848. (J and K) Quantification of neurite length (J) and apoptosis (K) of neurons cultured for 24 h in normal or conditioned medium with or without 100 μM R-848. In a separate culture, neurons grown in normal medium were first stimulated with 100 μM R-848 for 18 h, washed thoroughly to eliminate trace amounts of R-848, and further incubated in fresh normal medium for 12 h, after which the supernatant was collected as the conditioned medium. Statistical analysis was done by *t* test. *, $P < 0.05$; **, $P < 0.01$ versus controls (untreated, 0 μM or 0 h). Data are the mean ± the SEM for triplicate determinations. Bars: (A) 100 μm; (E) 50 μm.

R-848 functions only through TLR8 in neurons, as TLR7 is absent (Fig. 1 D). Primary neurites of neurons stimulated with R-848 for 24 h were significantly shorter in length (Fig. 2, A and B) and fewer in number (Fig. 2, A and C) compared with controls. A slight, but substantial, increase in neuronal death after R-848 exposure was observed by nuclear morphology (Fig. 2 D). Anticleaved caspase3 immunostaining suggested that the neuronal death was mediated by the classical effector caspase pathway (Fig. 2 E). A dose–response (Fig. 2, F and G) and time-course (Fig. 2, H and I) analysis revealed that the effects of R-848 on neurons were concentration-dependent and relatively slow. Corresponding results were obtained with R-848 treatment on more mature neurons replated from a 5-d-in vitro (DIV5) culture (Fig. S2, available at http://www.jcb.org/cgi/content/full/jcb.200606016/DC1). As controls, the exposure of neurons to lipopolysaccharide (LPS), which is a potent inducer of neuronal death in mixed CNS cultures through activation of TLR4 on microglia (Lehnardt et al., 2003), and to loxoribine, which is a TLR7-specific agonist (Heil et al., 2003), produced no detectable effect (Fig. 2, A–D), suggesting a lack of contaminating CNS immune cells in the culture and a selective role for TLR8 in the R-848–induced neuronal responses. The effects of R-848 did not appear to be mediated through soluble secreted factors because conditioned medium from R-848–stimulated cultures failed to affect morphology of freshly plated neurons (Fig. 2, J and K). Thus, R-848 specifically inhibits neurite outgrowth and triggers apoptosis in cultured neurons.

We noted that in R-848–stimulated cultures, ~13% of the cleaved caspase3-positive neurons exhibited neurite lengths comparable to those of untreated neurons, whereas 12% of the cleaved caspase3-negative neurons lacked processes (Fig. 3 A). This observation, as well as the similar timing for the onset of R-848–induced neurite outgrowth inhibition and apoptosis (Fig. 2, H and I), implies that these events are not necessarily sequential, but may result from two parallel processes. Therefore, we next addressed whether the effects of R-848 on neurons could be dissociated. Addition of a pan-caspase (unpublished data) or a caspase3-specific inhibitor (Z-DEVD-FMK) completely inhibited R-848–induced neuronal apoptosis (Fig. 3, B and C). Despite this elimination of the apoptotic response, R-848 stimulation still profoundly inhibited neurite outgrowth (Fig. 3, B and D), suggesting that R-848–induced inhibition of neurite outgrowth is not a consequence of apoptosis. Furthermore, removal of R-848 from the culture medium immediately before the appearance of the earliest morphological changes in neurons restored neurite outgrowth, but did not prevent apoptosis (Fig. 3, E and F). Collectively, these results suggest that R-848–induced neurite

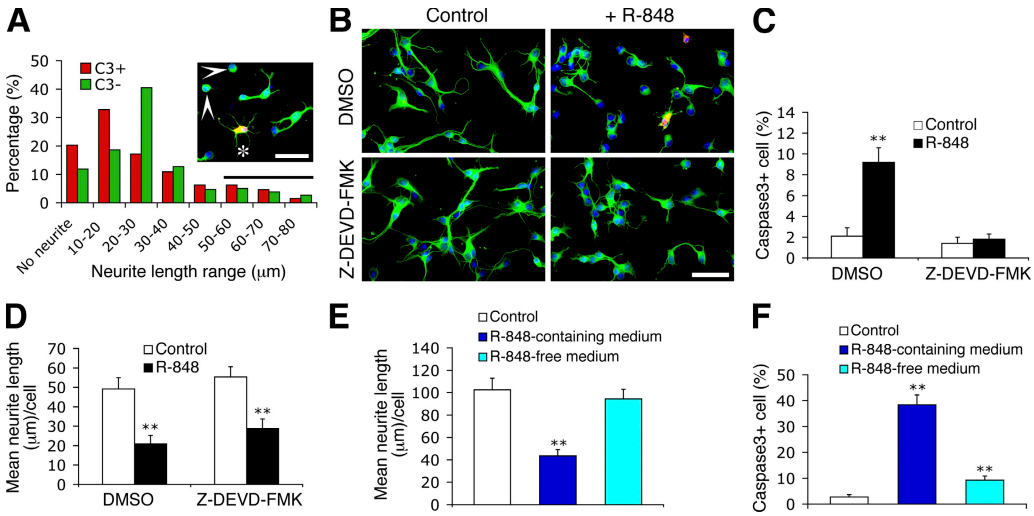

Figure 3. **Neurite outgrowth inhibition and neuronal apoptosis induced by R-848 are dissociable.** (A) Neurite length distribution of the cleaved caspase3-positive (C3+; $n = 64$) and the cleaved caspase3-negative neurons (C3−; $n = 338$) in cultures treated with 100 μM R-848 for 24 h. Cells with neurite length of <10 μm are defined as having no neurites, and cells with neurites longer than the average neurite length of the untreated neurons (56.4 ± 5.9 μm) are considered as having normal neurites (indicated by the horizontal bar). The insert shows a representative field of R-848–treated cultures. Asterisk and arrowheads indicate a C3+ cell with normal neurites and C3− cells with no neurites, respectively. Cells were fixed and double-immunostained with anti–βIII-tubulin (green) and anti-cleaved caspase3 (red) antibodies. (B) Representative micrographs of neurons untreated (control) or treated with 100 μM R-848 for 24 h in the presence of vehicle control (1% DMSO) or caspase3 inhibitor (20 μM Z-DEVD-FMK). (C and D) Quantification of the effects of blocking caspase3 activity on R-848–induced apoptosis (C) and neurite outgrowth inhibition (D). (E and F) Quantification of neurite length (E) and apoptosis (F) of neurons that were initially exposed to 100 μM R-848 for 12 h (the time when the R-848–induced morphological changes become detectable), then switched to R-848–free or –containing medium for a further incubation of 36 h. Control cultures were never exposed to R-848. Statistical analysis was done by *t* test. **, $P < 0.01$ versus controls. Data are the mean ± the SEM for triplicate determinations. Bars, 50 μm.

outgrowth inhibition and apoptosis likely occur independently of one another.

To determine whether TLR8, which is intracellularly localized in neurons (Fig. 1 E), specifically mediates the observed effects of R-848, we introduced an anti-TLR8 polyclonal antibody with validated specificity (Fig. S1 A) into freshly cultured neurons by using Chariot, which is a protein-transduction reagent previously demonstrated to deliver antibodies efficiently into postmitotic neurons (Coulpier et al., 2002). As protein delivery bypasses the transcription–translation process associated with conventional transfection techniques, it provides the opportunity to study early and rapidly proceeding cellular events, such as neurite outgrowth. Anti–TLR8-transduced neurons exhibited substantially longer neurite lengths (Fig. 4, A and B) and reduced apoptosis (Fig. 4, A and C) in response to R-848 compared with control IgG-transduced neurons. Similar results were obtained with an anti-TLR8 monoclonal antibody (unpublished data). The attenuating effect of anti-TLR8 antibody was abrogated by co-delivery of an inhibitory peptide specific to the antibody (unpublished data). These results show that R-848 inhibits neurite outgrowth and triggers apoptosis through TLR8. The partial blocking effect of anti-TLR8 antibody may be attributed to incomplete inhibition of TLR8, or alternatively, to the implication of other, yet unknown, mechanisms. R-848 was recently shown to activate caspase 1 in macrophages through cyropyrin/Nalp3 in a MAPK/NF-κB/TLR7-independent manner

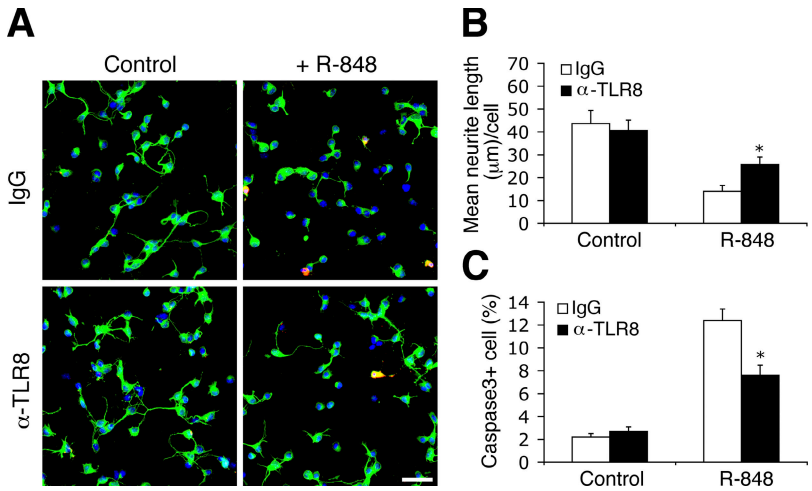

Figure 4. **R-848 effects on neurons are attenuated by a polyclonal antibody specifically against TLR8.** (A) Representative micrographs of nonimmune IgG- and anti-TLR8 (α-TLR8)–transduced neurons that were either untreated (control) or treated with 100 μM R-848 for 18 h. Cells were fixed and double-immunostained with anti–βIII-tubulin (green) and anti-cleaved caspase3 (red) antibodies. Bar, 50 μm. (B and C) Quantification of the anti-TLR8–mediated blocking effects on R-848–induced neurite outgrowth inhibition (B) and apoptosis (C). Statistical analysis was done by *t* test. *, $P < 0.05$ versus nonimmune IgG-transduced neurons treated with R-848. Data are the mean ± the SEM for triplicate determinations.

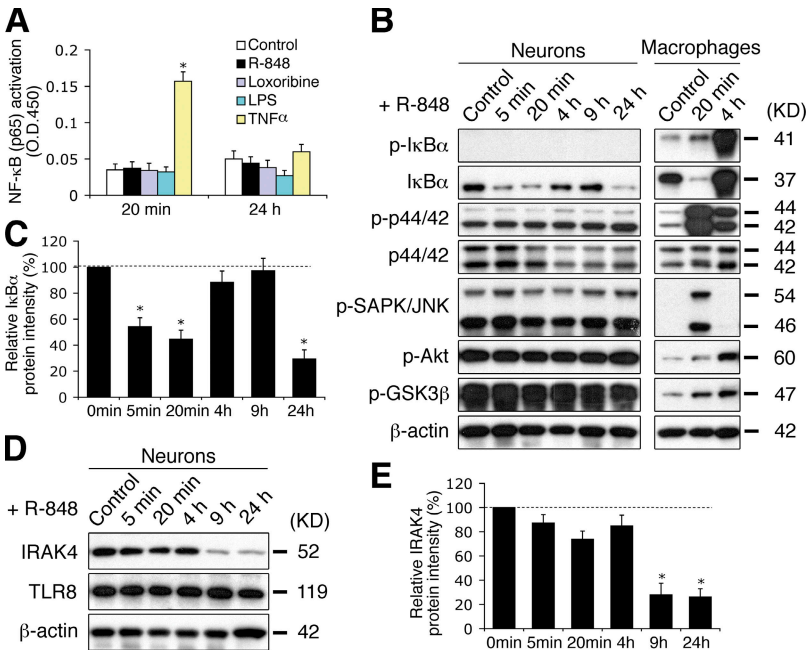

Figure 5. **TLR8 stimulation in neurons does not activate the canonical TLR–NF-κB signaling pathway, but rather down-regulates IκBα and IRAK4.** (A) ELISA assay for NF-κB (p65) transactivation using nuclear extracts from cortical neurons stimulated with 100 μM R-848, 500 μM loxoribine, 5 μg/ml LPS, or 10 ng/ml TNFα for the indicated times. LPS and TNFα serve as negative and positive controls, respectively. (B) Western blotting of the hallmarks of the conventional TLR-signaling pathway with lysates from neurons and Raw264.7 macrophages treated with 100 μM R-848 for the indicated times. (C) Quantification of changes in IκBα levels in R-848–stimulated neurons by band densitometry. A representative blot is shown in B. (D) Western blotting of IRAK4 in neurons stimulated with 100 μM R-848 for the indicated times. Note that TLR8 levels remain unchanged. (E) Quantification of changes in IRAK4 levels by band densitometry. A representative blot is shown in D. Data in C and E, expressed as percentage normalized to controls (100%), are the mean ± the SEM for pooled Western-blots from three independent cultures. Statistical analysis was done by *t* test. *, $P < 0.05$ versus controls.

(Kanneganti et al., 2006), and future work will determine whether this cyropyrin pathway mediates R-848 effects on neurons and if it relates to TLR8 signaling.

To dissect the mechanism underlying TLR8-activated neuronal responses, we investigated whether TLR8 in neurons signals through its conventional pathway, the MAPK and NF-κB cascades (Akira and Takeda, 2004). A highly sensitive ELISA-based analysis revealed that R-848 did not induce NF-κB (Fig. 5 A) or AP-1 (unpublished data) transactivation in cultured neurons. Furthermore, IκBα (Ser32) phosphorylation and other characteristic hallmarks of TLR signaling, including the phosphorylation of ERK1/2, SAPK/JNK, Akt, and GSK3β, were not detected in neurons (Fig. 5 B). In contrast, these signaling molecules were readily activated by R-848 in macrophages (Fig. 5 B). As additional evidence that neuronal TLR8 signaling occurs independently of the canonical TLR–MyD88–NF-κB pathway, MyD88 deficiency did not confer resistance to R-848 effects on the morphology of cultured neurons (unpublished data).

Interestingly, two essential components of the canonical TLR pathway, IκBα and interleukin 1 receptor–associated kinase 4 (IRAK4), were markedly down-regulated in cultured neurons after prolonged (9 h) R-848 stimulation (Fig. 5, B–E). A transient reduction of IκBα was also observed 5 min after R-848 administration (Fig. 5, B and C). The decrease of IκBα likely occurred through a previously described (O'Connor et al., 2005) phosphorylation-independent degradation process because IκBα (Ser32) phosphorylation was not detected in R-848–stimulated neurons (Fig. 5 B). Prolonged TLR stimulation was shown to cause IRAK4 degradation in macrophages (Hatao et al., 2004). Notably, the timing of the down-regulation of IκBα and IRAK4 coincided with the onset of R-848–induced neurite outgrowth inhibition and apoptosis (Fig. 2, H and I), suggesting a possible link between these events. IκBα may be important in neuronal TLR8 signaling, in light of its capacity to regulate gene transcriptional activity independent of NF-κB (Viatour et al., 2003). It is also interesting to note that a proapoptotic role has been recently suggested for IRAK4 (Salaun et al., 2006). R-848–induced down-regulation of IRAK4 may provide a feedback mechanism to prevent excessive neuronal death.

Our results suggest that, fundamentally different from in immune cells, TLR8 in neurons functions in a NF-κB–independent manner. Similarly, our work with neuron cultures from *Tlr3*-deficient mice suggests that TLR3 stimulation by polyinosinic-polycytidylic acid inhibits neurite extension, but does not activate NF-κB (unpublished data). As NF-κB activation has been implicated in promoting both neurite outgrowth and neuronal survival (Foehr et al., 2000), it is conceivable that TLR-signaling in neurons leading to neurite suppression and apoptosis does not involve the NF-κB pathway.

Although the physiological relevance of TLR8 in neurodevelopment is yet to be determined, its role may involve processes negatively regulating axonogenesis and neuron number in the developing nervous system, in light of the developmentally regulated expression of TLR8 in axons and neurons, as well as the capability of TLR8 to inhibit neurite outgrowth and induce neuronal apoptosis. Our findings also add important evidence supporting the emerging concept that traditional "immune molecules" may possess distinct functions in neuronal processes (Boulanger and Shatz, 2004).

Materials and methods

Animals

Swiss-Webster mice were obtained from Taconic Farms. All animal procedures were conducted in accord with the National Institutes of Health and the Harvard Medical School guidelines.

Chemicals and antibodies

R-848 was purchased from GL Synthesis; LPS was purchased from List Biological Laboratories; Z-DEVD-FMK was purchased from Biovision; loxoribine

was obtained from Invivogen; rabbit anti-TLR7 polyclonal antibody, rabbit anti-TLR8 polyclonal antibody, and synthetic inhibitory peptide were obtained from Invitrogen; rabbit anti-TLR4 and rabbit anti–NF-κB p65 (C-20) polyclonal antibodies were purchased from Santa Cruz Biotechnology, Inc.; rabbit anti-MyD88 polyclonal, mouse anti-neurofilament (200 kD) monoclonal, and mouse anti–MAP-2 monoclonal antibodies were obtained from CHEMICON International, Inc.; recombinant mouse TNFα, mouse anti–β-actin monoclonal antibody, cytosine arabinoside (Ara-C), and avertin (2,2,2-Tribromoethanol) were purchased from Sigma-Aldrich; mouse anti-neuronal class III β-tubulin (TUJ1) monoclonal antibody was obtained from Covance; rabbit anti-cleaved caspase3 (Asp175) monoclonal (5A1), rabbit anti-IκBα polyclonal, rabbit anti–phospho-IκBα (Ser32) polyclonal, rabbit anti-p44/42 MAPK polyclonal, rabbit anti–phospho-p44/42 (Thr202/Tyr204) polyclonal, rabbit anti–phospho-SAPK/JNK (Thr183/Tyr185) polyclonal, rabbit anti–phospho-Akt (Ser437) polyclonal, and rabbit anti-GSK3β (Ser9) polyclonal antibodies were obtained from Cell Signaling Technology; rabbit anti-IRAK4 polyclonal antibody was purchased from Millipore; goat anti–rabbit/mouse IgG-HRP was obtained from GE Healthcare; and goat anti–rabbit/mouse–FITC/Cy3 was purchased from Jackson ImmunoResearch Laboratories.

Whole-mount in situ hybridization

The nucleotide sequence CATGGATTCTGACGTGCTTTTGTCTGCTGTCCTCTGGAACCAGTGCCA located within the N terminus of mouse *Tlr8* (nt 81–128; GeneBank accession no. NM_133212) was selected as the probe, of which specificity was assessed by BLAST. The 48-bp oligonucleotide antisense and sense probes were synthesized and labeled with 10 optimally spaced DIG molecules by GeneDetect.com Ltd. Whole-mount in situ hybridization with E12–12.5 embryos was performed following the manufacturer's protocol. The anti–DIG-AP Fab fragment was purchased from Roche.

Primary neuron culture and stimulation

Neocortical neurons from mouse E16–17 embryos were prepared as previously described (Lehnardt et al., 2003). Typically, >97% cells generated from the procedure were neurons, as estimated by neuron-specific βIII-tubulin (TUJ1) staining. Cells were seeded at a density of 4×10^4 cells/well on poly-L-lysine–coated 12-mm coverslips or at a density of 2.5×10^6 cells/well on 6-well plates, and cultured in neurobasal medium (Invitrogen) supplemented with B-27 (Invitrogen), 0.5 mM L-glutamine, and 1% antibiotic/antimycotic solution. Neurons freshly cultured for 4 h or transduced with antibodies (see the following section) were treated with various stimuli and further incubated for the times indicated. When applicable, 20 μM Z-DEVD-FMK or 1% DMSO (vehicle control) was added into the culture 1 h before the application of R-848. For all assays, including ELISA, morphological, and Western blot analysis, every condition studied was performed in triplicate wells.

Chariot-mediated delivery of antibody

The antibody delivery procedure was performed with Chariot reagents (Active Motif) following the manufacturer's instructions. In brief, 2 μg anti-TLR8 polyclonal antibody or nonimmune IgG was incubated with 2 μl of the Chariot reagent for 30 min at RT. The formulated antibody–Chariot complex was then applied onto neurons (which had been grown for 4 h after isolation) for 4 h of incubation to allow antibody internalization. When needed, 2 μg inhibitory peptide specific to the anti-TLR8 polyclonal antibody was transduced together with the anti-TLR8 antibody. The antibody- or nonimmune IgG–transduced cells were either cultured under normal conditions or subjected to R-848 stimulation.

Preparation of lysates and Western blotting

For tissues, adult spleen or mouse brains at designated developmental stages were dissected out under a stereomicroscope from the timed-pregnant or postnatal mice. 3–20 brains (depending on stages) from the same developmental stage were pooled together to eliminate the discrepancy between individuals. For cell cultures, primary cortical neurons and Raw264.7 macrophages (American Type Culture Collection), which were untreated or treated with various stimuli, were collected at the times indicated. The collected tissues or cells were lysed in RIPA buffer (150 mM NaCl, 50 mM Tris, 1% NP-40, 0.25% sodium deoxycholate, and 1 mM EGTA) supplemented with protease inhibitor cocktail tablet (Roche) and phosphatase inhibitors sodium orthovanadate (1 mM) plus NaF (1 mM). The protein concentration was determined using a Bradford-based assay (Bio-Rad Laboratories). The equally loaded protein samples were separated by SDS-PAGE using 10–20% linear Criterion gels (Bio-Rad Laboratories) and then electro-transferred onto a polyvinylidene difluoride membrane (Bio-Rad Laboratories) at 4°C overnight. The membrane was incubated in blocking solution (5% nonfat dry milk and 0.1% Tween-20 in Tris-buffered saline) at RT for 1 h, and then incubated with primary antibodies diluted (anti-TLR8 polyclonal antibody 1:1,000; other primary antibodies 1:1,000–2,000) in the blocking solution at 4°C overnight, followed by a thorough washing procedure and subsequent incubation with HRP-conjugated goat anti–rabbit or goat anti–mouse IgG (1:4,000 dilution) at RT for 1 h. Finally, ECL Plus reagents (GE Healthcare) were applied onto the membrane to detect the antibody-bound bands according to the manufacturer's instruction, and the resultant chemiluminescent signals were visualized with Kodak X-OMAT film (Kodak). Band densitometry was performed using IPLab3.5 software (Scanalytics) for Western-blots from three independent experiments.

Preparation of nuclear extracts and ELISA assay of NF-κB activation

Nuclear fractions from the stimulated neurons were prepared using the Nuclear Extract kit (Active Motif), and NF-κB assay was performed using the TransAM ELISA kit (Active Motif) according to the manufacture's protocols. In brief, 5 μg nuclear proteins were incubated in a 96-well plate coated with the oligonucleotide containing the NF-κB–binding sequence (5′-GGGACTTTCC-3′). The activated transcription factor specifically bound to the immobilized oligonucleotide was detected using the antibody against p65 and followed by HRP-conjugated secondary antibody detection. The color-developing solution was applied in the sample wells, and the absorbance was quantified at 450 nm by spectrophotometry using a microplate reader (Spectra MAX250; Molecular Devices).

Immunohistochemistry and immunocytochemistry

For tissues, whole embryos or embryonic brains were dissected out and fixed by immersion in 4% PFA overnight at 4°C. Postnatal and adult mice were perfused transcardially with 4% PFA after anesthetization with avertin, and tissues were subsequently removed and postfixed overnight at 4°C. The collected tissues were then embedded in paraffin and cut into 5-μm-thick sagittal sections, which were deparaffinized using a standard histology protocol immediately before immunohistochemical staining. For cultures, cells grown on coverslips were fixed with either methanol for 10 min at –20°C or 4% PFA for 10 min at RT for immunocytochemistry. In the staining procedure, tissue sections or cell coverslips were permeabilized with 0.5% Triton X-100 (Sigma-Aldrich) for 10 min, and then blocked with the buffer containing 10% normal goat serum (Sigma-Aldrich), 1% (wt/vol) BSA, and 0.2% (vol/vol) Triton X-100 for 2 h at RT, followed by incubation with primary antibodies that were diluted (anti-TLR8 polyclonal and anti-neurofilament 200 kD monoclonal antibodies 1:50 for immunohistochemistry, 1:100 for immunocytochemistry; anti-MAP2 monoclonal antibody 1:50; and anti-βIII-tubulin and anti-cleaved caspase3 monoclonal antibodies 1:100) in the dilution buffer (2% normal goat serum, 1% BSA, and 0.1% Triton X-100) overnight at 4°C. Samples were subsequently incubated with FITC- and/or Cy3-conjugated species-specific secondary antibody/antibodies in the dilution buffer (1:200 dilution) for 1 h at RT. VECTASHIELD Mounting Medium with DAPI (Vector Laboratories) was used to mount the fluorescently labeled samples and to stain cell nuclei.

Microscopic imaging analysis

The stained sections or coverslips were visualized and the images were digitally acquired using a fluorescence microscope (Eclipse 660; Nikon) equipped with a Spot cooled charge-coupled device camera (Diagnostic Instruments). In some cases, a confocal microscope (LSM510; Carl Zeiss MicroImaging, Inc.) was used.

To evaluate apoptosis, images were captured with a 10× objective lens (Plan Fluor; Nikon) in an unbiased manner. As the majority of cells that display condensed nuclei (visualized by DAPI), which is a characteristic morphology of apoptotic cells, were clearly stained by anti-cleaved caspase3 (Asp175) monoclonal (5A1) antibody, the rate of apoptosis was expressed as the percentage of the cleaved caspase3-positive cells relative to the total cells within a given field (300–400 cells/field). The apoptosis rate presented in the figures was obtained as a mean from 12 fields randomly chosen from the triplicate wells of each condition studied ($n = 12$ fields).

To determine neurite outgrowth, images were acquired with a 20× objective lens (Plan Fluor; Nikon) from two randomly chosen fields in each well, triplicate wells of every condition. Neuron-specific βIII-tubulin (TUJ1) and the cleaved caspase3 were stained to visualize the neuronal somata and processes and to identify the apoptotic cells, respectively. Unless indicated, only the neurites of the cleaved caspase3-negative cells were used for measurement to eliminate the impact of the apoptotic cell

morphology on the outcome of statistical analysis for neurite parameters. A primary neurite was defined as a process extending from the cell body by at least one cell diameter (~10 μm). The primary neurites of nonapoptotic cells were individually traced using Spot software (Version 4.6) with the Curve tool for 20–30 cells within a given field for all fields acquired for every condition (n = 100–180 cells/condition). The length of individual neurites was automatically calculated according to the calibrated scales using the same software. The total number of the measured primary neurites was counted. The measurement data were then exported into Excel 2003 (Microsoft) for statistical analysis. The average neurite length and neurite number were obtained by dividing the total neurite length and total number of neurites, respectively, by the total number of the cleaved caspase3-negative cells (including cells bearing no neurites) measured for each condition.

Representative images shown in the figures were modified using the Level tool in Photoshop (Adobe) to enhance detail and contrast. The same adjustment was applied over the image as a whole for all original images.

Statistical analysis

The significance of difference for quantitative analysis was assessed by pair-wise comparisons with *t*-test. Data are presented as the mean ± the SEM. Unless indicated, all cell culture experiments were performed with samples from three independent cell preparations.

Online supplemental material

Fig. S1 shows the specificity of the affinity-purified anti-TLR8 polyclonal antibody and the axon-specific expression of TLR8 in the embryonic brain. Fig. S2 shows that R-848 inhibits neurite outgrowth and triggers apoptosis in neurons developed in vitro. There is also a Supplemental materials and methods. Online supplemental material is available at http://www.jcb.org/cgi/content/full/jcb.200606016/DC1.

We thank M. Anderson for comments on the manuscript and W. Cardoso for assistance on the whole-mount in situ hybridization.

This study was supported by grants from the National Institutes of Health (PO1NS038475) and the National Multiple Sclerosis Society (RG3426A2/1) to T. Vartanian.

Submitted: 5 June 2006
Accepted: 11 September 2006

References

Akira, S., and K. Takeda. 2004. Toll-like receptor signalling. *Nat. Rev. Immunol.* 4:499–511.

Belvin, M.P., and K.V. Anderson. 1996. A conserved signaling pathway: the *Drosophila* toll-dorsal pathway. *Annu. Rev. Cell Dev. Biol.* 12:393–416.

Boulanger, L.M., and C.J. Shatz. 2004. Immune signalling in neural development, synaptic plasticity and disease. *Nat. Rev. Neurosci.* 5:521–531.

Coulpier, M., J. Anders, and C.F. Ibanez. 2002. Coordinated activation of autophosphorylation sites in the RET receptor tyrosine kinase: importance of tyrosine 1062 for GDNF mediated neuronal differentiation and survival. *J. Biol. Chem.* 277:1991–1999.

Du, X., A. Poltorak, Y. Wei, and B. Beutler. 2000. Three novel mammalian toll-like receptors: gene structure, expression, and evolution. *Eur. Cytokine Netw.* 11:362–371.

Foehr, E.D., X. Lin, A. O'Mahony, R. Geleziunas, R.A. Bradshaw, and W.C. Greene. 2000. NF-kappa B signaling promotes both cell survival and neurite process formation in nerve growth factor-stimulated PC12 cells. *J. Neurosci.* 20:7556–7563.

Hatao, F., M. Muroi, N. Hiki, T. Ogawa, Y. Mimura, M. Kaminishi, and K. Tanamoto. 2004. Prolonged Toll-like receptor stimulation leads to down-regulation of IRAK-4 protein. *J. Leukoc. Biol.* 76:904–908.

Heil, F., P. Ahmad-Nejad, H. Hemmi, H. Hochrein, F. Ampenberger, T. Gellert, H. Dietrich, G. Lipford, K. Takeda, S. Akira, et al. 2003. The Toll-like receptor 7 (TLR7)-specific stimulus loxoribine uncovers a strong relationship within the TLR7, 8 and 9 subfamily. *Eur. J. Immunol.* 33:2987–2997.

Hoffmann, J.A. 2003. The immune response of *Drosophila*. *Nature*. 426:33–38.

Hoffmann, J.A., F.C. Kafatos, C.A. Janeway, and R.A. Ezekowitz. 1999. Phylogenetic perspectives in innate immunity. *Science*. 284:1313–1318.

Jurk, M., F. Heil, J. Vollmer, C. Schetter, A.M. Krieg, H. Wagner, G. Lipford, and S. Bauer. 2002. Human TLR7 or TLR8 independently confer responsiveness to the antiviral compound R-848. *Nat. Immunol.* 3:499.

Kanneganti, T.D., N. Ozoren, M. Body-Malapel, A. Amer, J.H. Park, L. Franchi, J. Whitfield, W. Barchet, M. Colonna, P. Vandenabeele, et al. 2006. Bacterial RNA and small antiviral compounds activate caspase-1 through cryopyrin/Nalp3. *Nature*. 440:233–236.

Kielian, T. 2006. Toll-like receptors in central nervous system glial inflammation and homeostasis. *J. Neurosci. Res.* 83:711–730.

Lehnardt, S., L. Massillon, P. Follett, F.E. Jensen, R. Ratan, P.A. Rosenberg, J.J. Volpe, and T. Vartanian. 2003. Activation of innate immunity in the CNS triggers neurodegeneration through a Toll-like receptor 4-dependent pathway. *Proc. Natl. Acad. Sci. USA*. 100:8514–8519.

O'Connor, S., S. Markovina, and S. Miyamoto. 2005. Evidence for a phosphorylation-independent role for Ser 32 and 36 in proteasome inhibitor-resistant (PIR) IkappaBalpha degradation in B cells. *Exp. Cell Res.* 307:15–25.

Prehaud, C., F. Megret, M. Lafage, and M. Lafon. 2005. Virus infection switches TLR-3-positive human neurons to become strong producers of beta interferon. *J. Virol.* 79:12893–12904.

Roach, J.C., G. Glusman, L. Rowen, A. Kaur, M.K. Purcell, K.D. Smith, L.E. Hood, and A. Aderem. 2005. The evolution of vertebrate Toll-like receptors. *Proc. Natl. Acad. Sci. USA*. 102:9577–9582.

Rose, D., X. Zhu, H. Kose, B. Hoang, J. Cho, and A. Chiba. 1997. Toll, a muscle cell surface molecule, locally inhibits synaptic initiation of the RP3 motoneuron growth cone in *Drosophila*. *Development*. 124:1561–1571.

Salaun, B., I. Coste, M.C. Rissoan, S.J. Lebecque, and T. Renno. 2006. TLR3 can directly trigger apoptosis in human cancer cells. *J. Immunol.* 176:4894–4901.

Viatour, P., S. Legrand-Poels, C. van Lint, M. Warnier, M.P. Merville, J. Gielen, J. Piette, V. Bours, and A. Chariot. 2003. Cytoplasmic IkappaBalpha increases NF-kappaB-independent transcription through binding to histone deacetylase (HDAC) 1 and HDAC3. *J. Biol. Chem.* 278:46541–46548.

Wadachi, R., and K.M. Hargreaves. 2006. Trigeminal nociceptors express TLR-4 and CD14: a mechanism for pain due to infection. *J. Dent. Res.* 85:49–53.

Ma et al., http://www.jcb.org/cgi/content/full/jcb.200606016/DC1

Cell culture and transfection

HEK293T and Raw264.7 macrophage (American Type Culture Collection) cell lines were maintained in DME supplemented with 10% fetal calf serum at 37°C/5% CO_2. Transient transfection of HEK293T cells with the plasmid harboring the full-length mouse *Tlr8* cDNA (pTLR8-HA) fused to a HA epitope at the 3′ terminus was performed with Lipofectamine2000 reagent (Invitrogen) according to the manufacturer's protocol. HEK293T cells were grown for 24 h after the transfection procedure, and were subsequently either fixed with 4% PFA for immunofluorescent detection or lysed in RIPA buffer (150 mM NaCl, 50 mM Tris, 1% NP-40, 0.25% sodium deoxycholate, and 1 mM EGTA) supplemented with a protease inhibitor cocktail tablet (Roche) and the phosphatase inhibitors sodium orthovanadate (1 mM) and NaF (1 mM) for Western blot analysis. Raw264.7 macrophages cultured on 12-mm coverslips were fixed for confocal immunofluorescence detection, and macrophages cultured on 6-well plates were treated with 100 μM R-848 for the indicated times, and then lysed for Western blot analysis.

Primary neuron replating and stimulation

Neocortical neurons were isolated from mouse E16–17 embryos and cultured in neurobasal medium (Invitrogen) supplemented with B-27 (Invitrogen), 0.5 mM L-glutamine, and 1% antibiotic/antimycotic solution. 5 μM Ara-C was added into the culture medium after 2 d to eliminate proliferating glial cells. Neurons cultured for 5 d were detached by incubation with 0.25% Trypsin-EDTA solution (Invitrogen) for 5–10 min. The detached cells were centrifuged and the cell pellet was collected, washed, suspended, and subsequently cultured in the DME/F-12 (1:1) medium supplemented with 10% fetal calf serum at a density of 1×10^5 cells/well. After 2 h of cell attachment, the replated neurons were washed twice and the medium was replaced with the aforementioned neurobasal medium containing 100 μM R-848. Neurons were further grown for 18 h, and then fixed with 4% PFA and double immunostained with anti–βIII-tubulin and anticleaved caspase3 monoclonal antibodies for the morphological analysis.

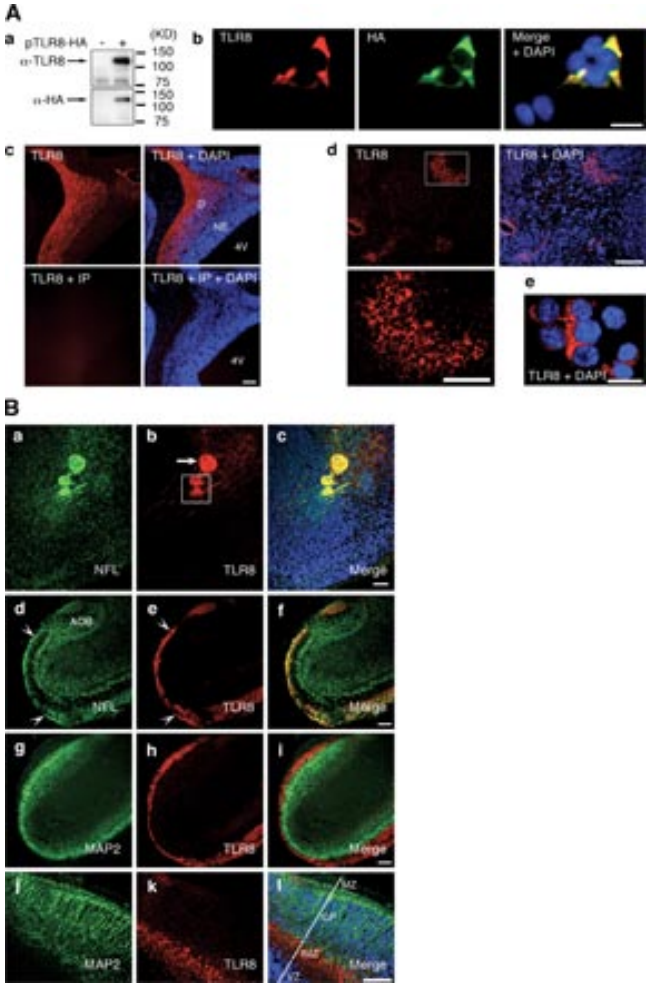

Figure S1. Specificity of the affinity-purified anti-TLR8 polyclonal antibody and the axon-specific expression of TLR8 in the embryonic brain. (A) Antibody specificity. (A, a) Western blot analysis using lysates from HEK cells transfected with a construct harboring full-length mouse *Tlr8* cDNA fused at the C terminus with an HA-tag (pTLR8-HA) shows that the antibody specifically recognizes the exogenously introduced TLR8 (arrows). The lower bands are nonspecific blotting products. (A, b) Immunocytochemistry shows that only cells (HEK) transfected with pTLR8-HA are stained, whereas the fluorescent signal is absent from the adjacent untransfected cells. Cell nuclei were visualized with DAPI staining (blue). (A, c) Immunohistochemistry on sagittal sections of E12 mouse brain shows that the differentiating field (D), but not the neuroepithelium (NE), of ventral mesencephalon and rhombencephalon is distinctly stained by anti-TLR8 (top row). The immunoreactivity of anti-TLR8 is abrogated by preincubation of the antibody with a synthetic inhibitory peptide (IP) specific to the antibody (bottom row). (A, d) The selective immunostaining pattern of anti-TLR8 in the adult spleen (a tissue known to express TLR8) constitutes a supportive evidence for antibody specificity. (bottom) Higher magnification view of the region framed in the top right image. (A, e) Confocal microscopic imaging shows intracellular localization of TLR8 in Raw264.7 macrophages (a cell line known to express TLR8). (B) Double-immunohistochemical staining with the anti-TLR8 polyclonal antibody and neuronal markers reveals axon-specific distribution of TLR8 in sagittal sections of E18 anterior commissure and fornix (B, a-c), olfactory bulb (B, d-i), and cerebral cortex (B, j-l). (B, a-c) TLR8 is highly expressed in the anterior commissure (frame) and fornix (arrow) and is colocalized with the axon-specific marker neurofilament 200 kD (NFL). (B, d-f) TLR8 is colocalized with NFL in the olfactory nerve layer (arrowheads), axons coming from neurons in the nasal epithelium to the olfactory bulb. (B, g-i) Double immunolabeling with the dendritic marker MAP2 shows that TLR8 is absent from the dendrites of olfactory neurons. (B, j-l) TLR8 is highly expressed in the cerebral intermediate zone where developing thalamocortical and cortifugal axons are enriched, and is apparently absent in the somata and dendrites of developing neurons within the cortical plate, as identified by MAP2 staining. 4V, 4th ventricle; AOB, accessory olfactory bulb; CP, cortical plate; IMZ, intermediate zone; MAP2, microtubule-associated protein 2; MZ, marginal zone; VZ, ventricular zone. Bars: (A, b and e) 20 μm; (A, d [bottom]) 50 μm; (A, c and d [top row]) 100 μm; (B) 100 μm.

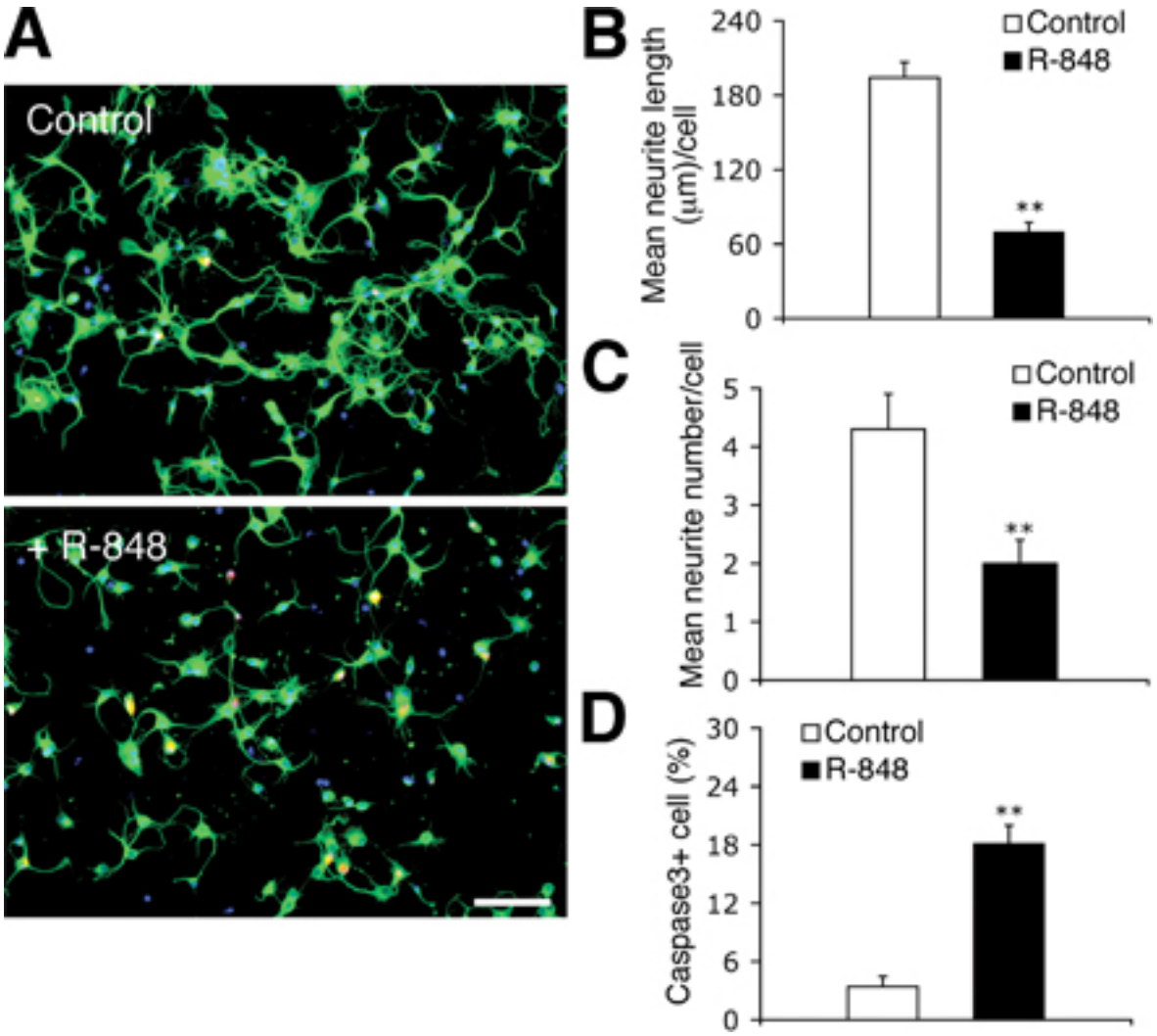

Figure S2. R-848 inhibits neurite outgrowth and triggers apoptosis in neurons developed in vitro. Cortical neurons were replated from a 5-d (DIV5) culture and grown for 18 h in the absence (control) or presence of 100 μM R-848. (A) Representative micrographs of untreated or treated neurons. Cells were fixed and double immunostained with anti-βIII-tubulin (green) and anticleaved caspase3 (red) monoclonal antibodies. Bar, 100 μm. (B-D) Quantification shows that neurite length (B) and neurite number (C) were reduced, whereas apoptosis (D) was markedly increased in neurons stimulated with R-848. Statistical analysis was done by *t* test. **, $P < 0.01$ versus control. Data are the mean ± the SEM for triplicate determinations. Similar results were obtained from two independent experiments.